

Electronic Supplementary Information

Assembly of single molecular magnets from dinuclear to 2D Dy-compounds with significant change of relaxation energy barriers

Zhi Chen,^a Ming Fang,^b Xiao-Min Kang,^a Yin-Ling Hou,^a Bin Zhao^{*,a}

Zhi Chen and Ming Fang have the same contribution to this paper.

a Department of Chemistry, Key Laboratory of Advanced Energy Material Chemistry, MOE, and Collaborative Innovation Center of Chemical Science and Engineering (Tianjin), Nankai University, Tianjin 300071, China. E-mail: zhaobin@nankai.edu.cn

b Department of Chemistry, Hebei Normal University of Science & Technology, Qinhuangdao 066004, Hebei province, P. R.China.

Materials and physical techniques.

All reagents and solvents employed were commercially available and used as received without further purification. Analyses for C, H and N were carried out on a elemental vario EL elemental analyzer. The FT-IR spectra were measured with a Bruker Tensor 27 Spectrophotometer on KBr disks. Powder X-ray diffraction measurements were recorded on a D/Max-2500 X-ray diffractometer using CuK α radiation. The magnetic properties were measured on a Quantum Design MPMS-XL7 and a PPMS-9 ACMS magnetometer. Diamagnetic corrections were made with Pascal's constants for all the constituent atoms.

Crystallographic studies

Diffraction intensity data for single crystals of **1** and **2** were collected on a Bruker Smart CCD diffractometer and a Rigaku 007 CCD diffractometer respectively, equipped with graphite monochromated MoK α radiation ($\lambda = 0.71073 \text{ \AA}$). The crystal was kept at 113.0 K during data collection. Using Olex2 [1], the structure was solved with the ShelXS [2] structure solution program using Direct Methods and refined with the ShelXL [3] refinement package using Least Squares minimisation.

The crystallographic data for **1** and **2** are listed in Table S1. CCDC 1407596 and 1407597 for **1** and **2** can be obtained free of charge from the Cambridge Crystallographic Data Centre (www.ccdc.cam.ac.uk/data_request/cif).

1. O. V. Dolomanov, L. J. Bourhis, R. J. Gildea, J. A. K. Howard and H. Puschmann, OLEX2: a complete structure solution, refinement and analysis program. *J. Appl. Cryst.* 2009, 42, 339-341.
2. SHELXS-97 (Sheldrick, 1990).
3. SHELXL, G.M. Sheldrick, *Acta Cryst.* 2008, A64, 112-122.

Synthesis of Dy₂(TA)₆(bipy)₂ (**1**)

The mixture of HTA (0.3 mmol, 51.7 mg), Dy(NO₃)₃·6H₂O (0.1 mmol, 45.7 mg), bipy (0.2 mmol, 31.2 mg), and 10 mL water heated in 25 mL teflon cup at 160°C for 3 days, and then cooled to room temperature at a rate of 2 °C h⁻¹. The block colorless crystals of **1** were collected in 46% yield, based on Dy after washed by water. Elemental analysis for **1**, Calc(%):C, 42.89; H, 2.45; N, 4.00. Found(%): C, 42.68; H, 2.83; N, 3.99. IR (KBr): 3420 m, 3090 m, 1626 s, 1552 s, 1524 s, 1476 m, 1423 s, 1392 s, 1344 m, 1223 m, 1176 w, 1156 m, 1126 m, 1063 w, 1034 m, 1014m, 859 m, 816 s, 794 s, 773 s, 738 m, 716 s, 654 m, 524 w, 425 s cm⁻¹.

Synthesis of [Dy₂(TDA)₃(bipy)₂(H₂O)₂]·bipy·2H₂O (**2**)

The mixture of H₂TDA (0.3 mmol, 51.7 mg), Dy₂O₃ (0.1 mmol, 33.6 mg), bipy (0.2 mmol, 31.2 mg), and 10 mL water heated in 25 mL teflon cup at 160°C for 3 days, and then cooled to room temperature at a rate of 2 °C h⁻¹. The block light brown crystals of **2** were collected in 37% yield, based on Dy after washed by water. Elemental analysis for **2**, Calc(%):C, 41.90; H, 2.78; N, 6.11. Found(%): C, 41.09; H, 3.05; N, 5.87. IR (KBr): 3161 s, 1650 s, 1563 s, 1524 s, 1478 m, 1461 w, 1439 m, 1374 s, 1177 w, 1157 m, 1062 w, 1014 m, 847 w, 773 s, 758 s, 738 m, 644 m, 472 s cm⁻¹.

Table S1 Crystal data and structure refinement for compound **1** and **2**.

Compound	1	2
Empirical formula	C ₅₀ H ₃₄ Dy ₂ N ₄ O ₁₂ S ₆	C ₄₈ H ₃₈ Dy ₂ N ₆ O ₁₆ S ₃
Formula weight	1400.23	1376.02
Temperature/K	113	294.15
Crystal system	monoclinic	triclinic
Space group	<i>P</i> 2 ₁ / <i>c</i>	<i>P</i> -1
<i>a</i> /Å	13.905(4)	10.1980(11)
<i>b</i> /Å	15.277(5)	11.0008(12)
<i>c</i> /Å	26.166(6)	12.5285(14)
<i>α</i> /°	90	78.936(2)
<i>β</i> /°	111.889(12)	87.716(2)
<i>γ</i> /°	90	63.320(2)
Volume/Å ³	5158(3)	1230.8(2)
<i>Z</i>	4	1

$\rho_{\text{calc}}/\text{cm}^3$	1.803	1.856
μ/mm^{-1}	3.184	3.218
$F(000)$	2744.0	676.0
Radiation	MoK α ($\lambda = 0.71075$)	MoK α ($\lambda = 0.71073$)
2θ range for data collection/ $^\circ$	3.65 to 50.018	3.316 to 50.014
Index ranges	$-16 \leq h \leq 16$, $-18 \leq k \leq 17$, $-31 \leq l \leq 31$	$-12 \leq h \leq 9$, $-13 \leq k \leq 13$, $-12 \leq l \leq 14$
Reflections collected	41908	6302
Independent reflections	9062 [$R_{\text{int}} = 0.0665$]	4292 [$R_{\text{int}} = 0.0190$]
Data/restraints/parameters	9062/62/699	4292/110/396
Goodness-of-fit on F^2	1.032	1.067
Final R indexes [$I \geq 2 \sigma(I)$]	$R_1 = 0.0377$, $wR_2 = 0.0904$	$R_1 = 0.0257$, $wR_2 = 0.0581$
Final R indexes [all data]	$R_1 = 0.0435$, $wR_2 = 0.0937$	$R_1 = 0.0321$, $wR_2 = 0.0622$
Largest diff. peak/hole / $e \text{ \AA}^{-3}$	1.60/-1.21	0.62/-0.54

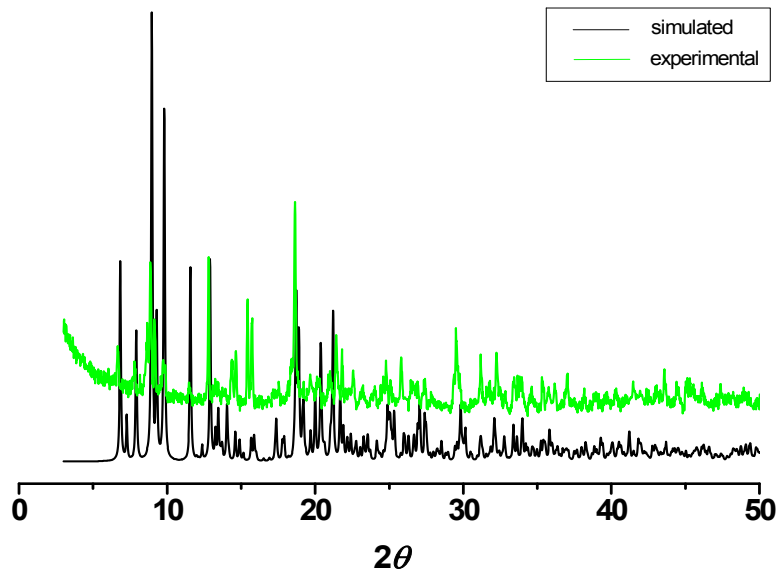


Fig. S1 The simulated and experimental PXRD patterns for **1**.

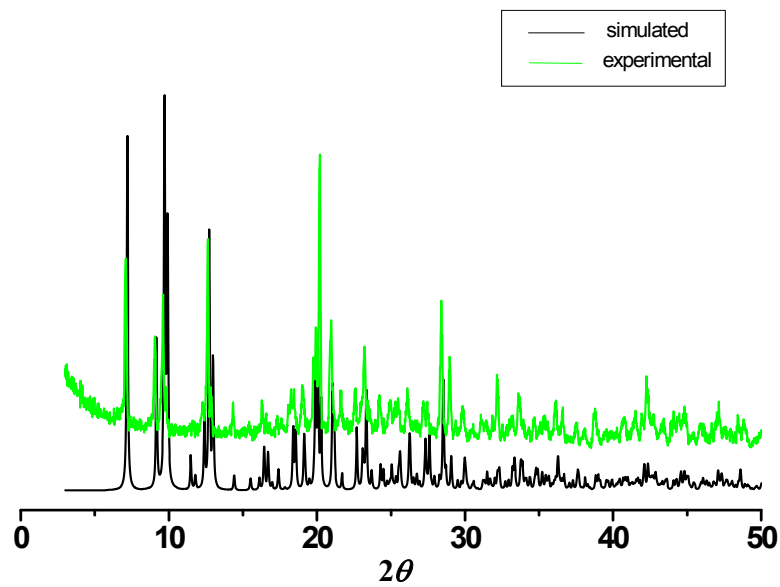


Fig. S2 The simulated and experimental PXRD patterns for 2.

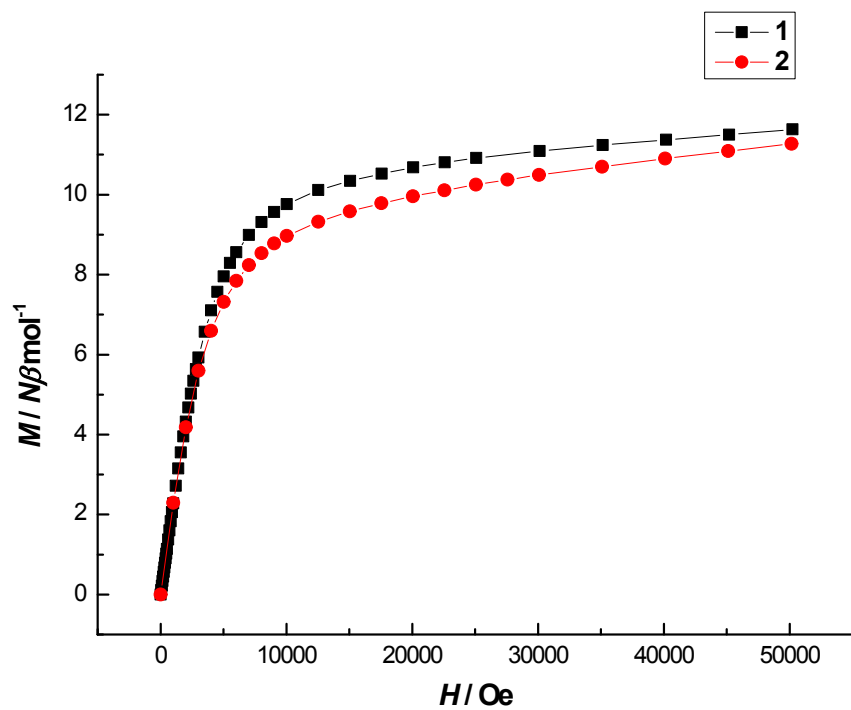


Fig. S3 M vs H plots at 2 K for complexes 1 and 2.

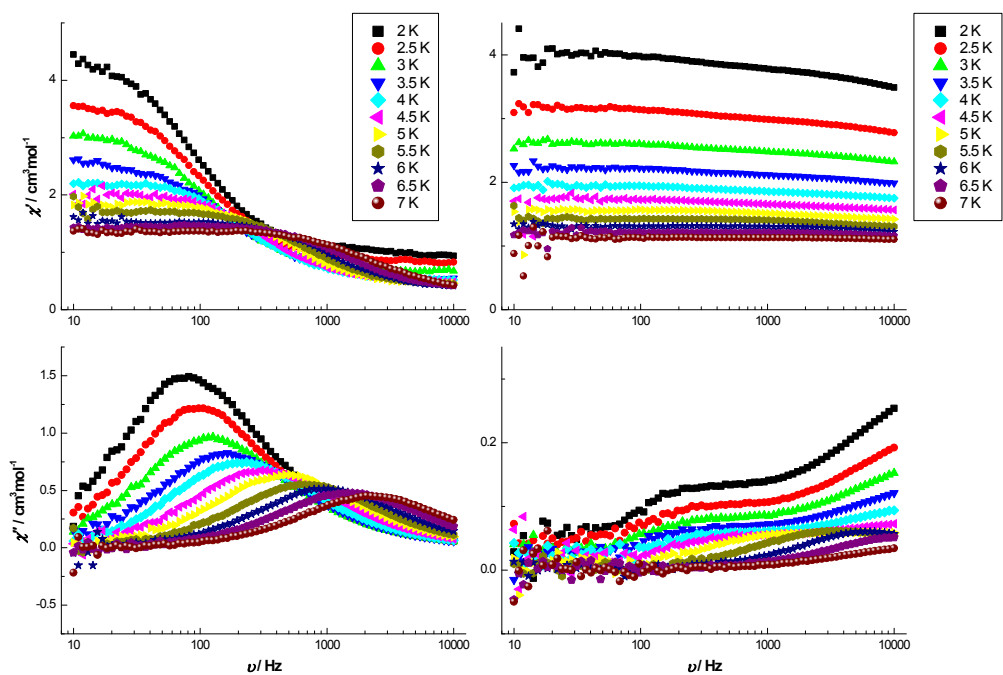


Fig. S4 Frequency dependences of the in-phase (χ_M') and out-of-phase (χ_M'') ac magnetic susceptibility for complexes **1** and **2** under zero dc field at 2-7 K.

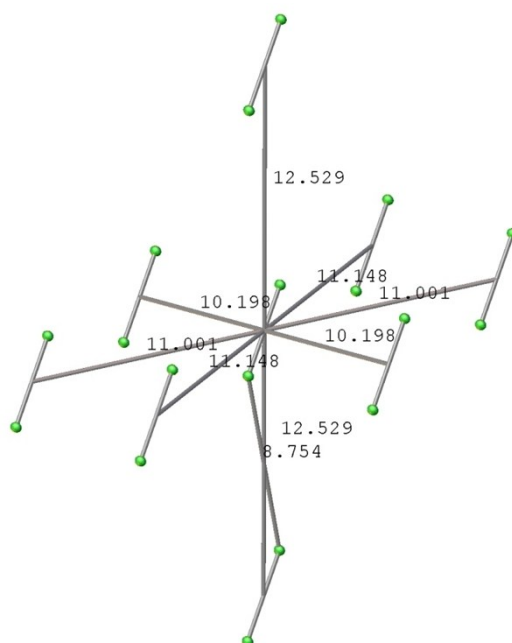


Fig. S5 The distances of dinuclear Dy units in compound **2**.

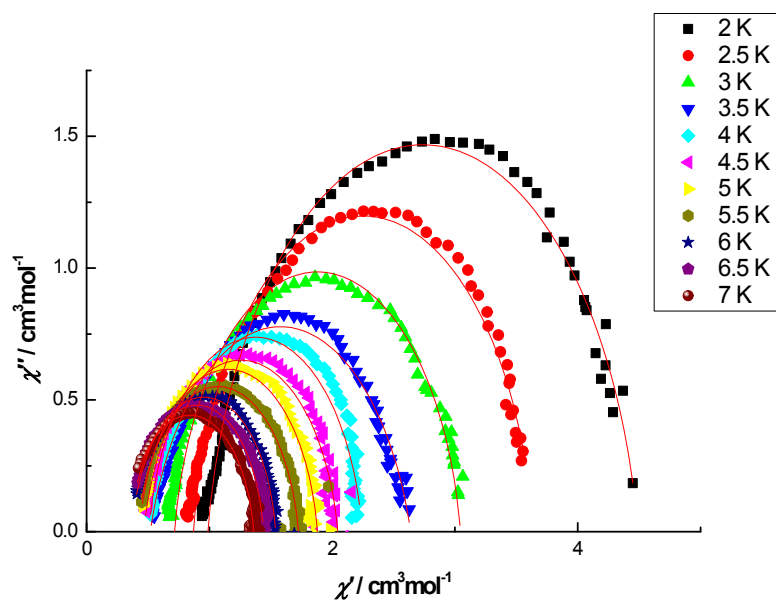


Fig. S6 The cole-cole plots at different temperatures for complex **1**. Red solid lines represent the least-squares fitting results obtained with a Debye model.

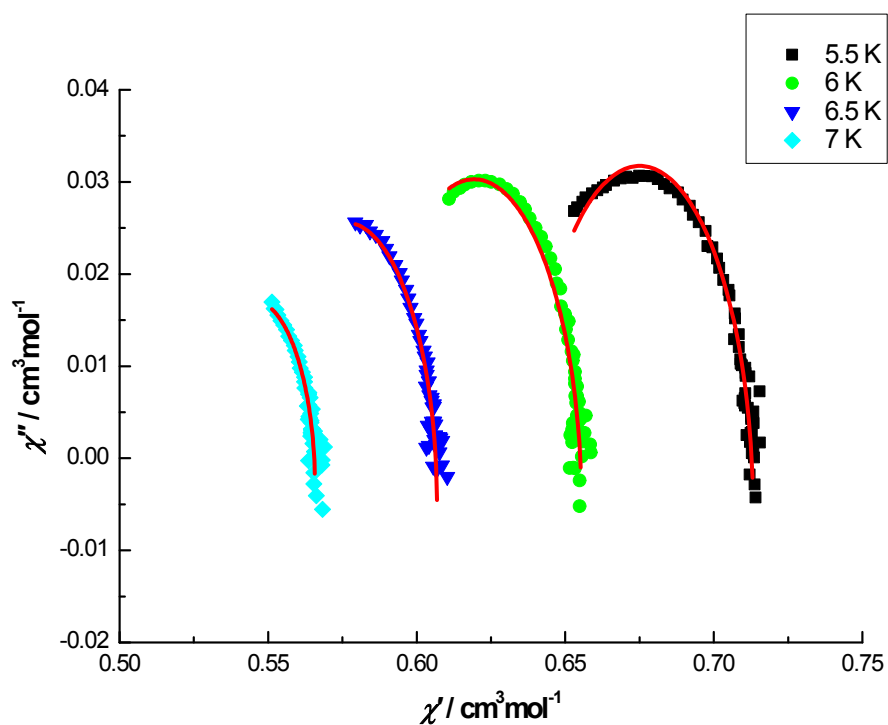


Fig. S7 The cole-cole plots at different temperatures for complex **2**. Red solid lines represent the least-squares fitting results obtained with a Debye model, with $\alpha = 0.10$ for all four fitting.

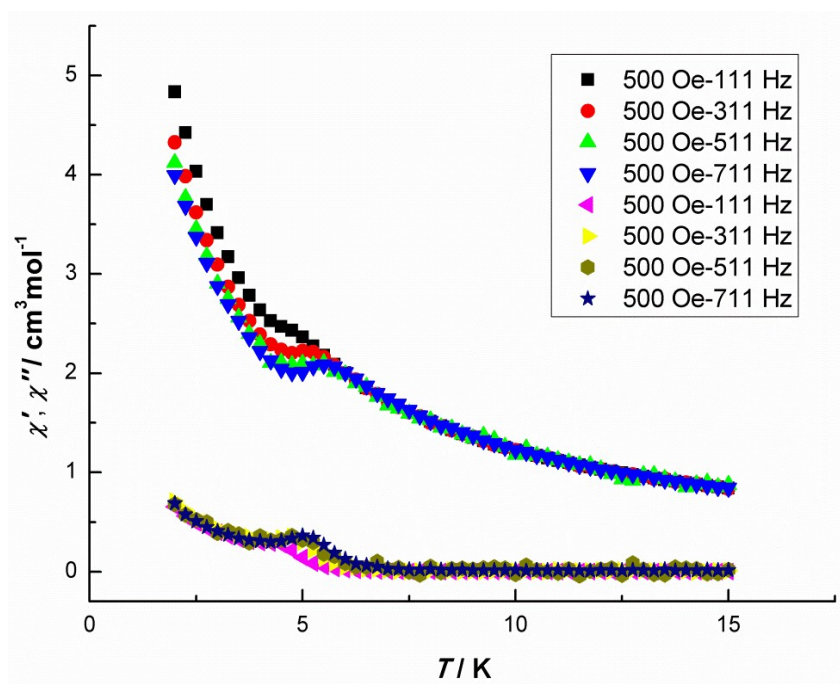


Fig. S8 AC magnetic susceptibilities the in-phase (χ_M') and out-of-phase (χ_M'') data under 500 Oe dc field for **2**.

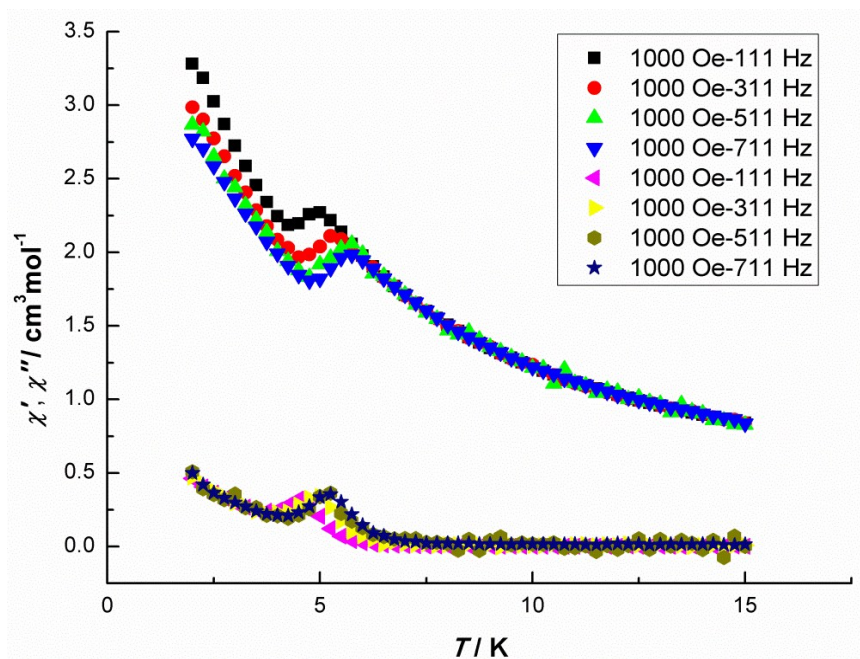


Fig. S9 AC magnetic susceptibilities the in-phase (χ_M') and out-of-phase (χ_M'') data under 1000 Oe dc field for **2**.

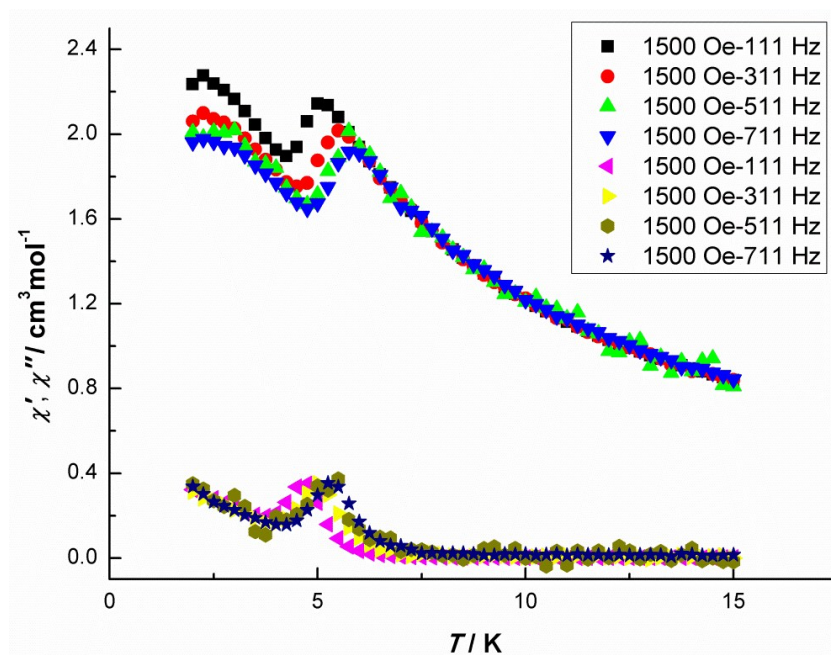


Fig. S10 AC magnetic susceptibilities the in-phase (χ_M') and out-of-phase (χ_M'') data under 1500 Oe dc field for **2**.

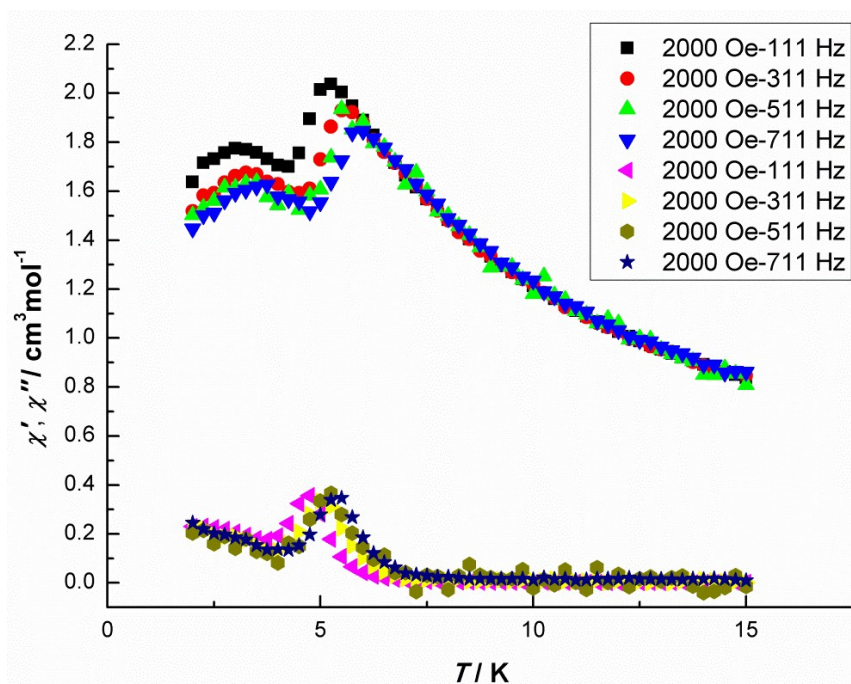


Fig. S11 AC magnetic susceptibilities the in-phase (χ_M') and out-of-phase (χ_M'') data under 2000 Oe dc field for **2**.

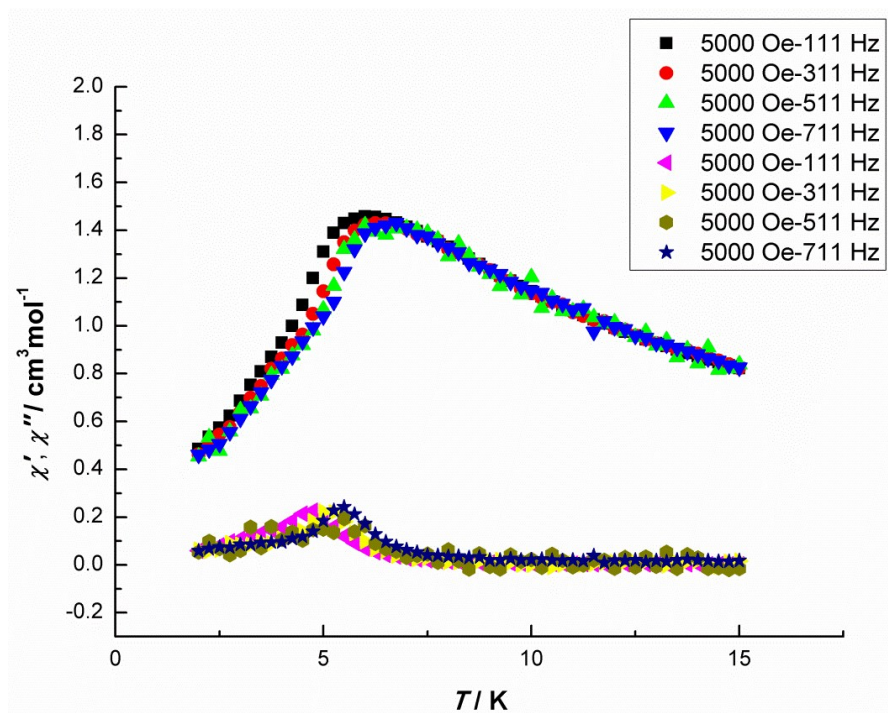


Fig. S12 Ac magnetic susceptibilities the in-phase ($\chi_{M'}$) and out-of-phase ($\chi_{M''}$) data under 5000 Oe dc field for **2**.